

Dalton Transactions

Accepted Manuscript



This is an *Accepted Manuscript*, which has been through the Royal Society of Chemistry peer review process and has been accepted for publication.

Accepted Manuscripts are published online shortly after acceptance, before technical editing, formatting and proof reading. Using this free service, authors can make their results available to the community, in citable form, before we publish the edited article. We will replace this *Accepted Manuscript* with the edited and formatted *Advance Article* as soon as it is available.

You can find more information about *Accepted Manuscripts* in the [Information for Authors](#).

Please note that technical editing may introduce minor changes to the text and/or graphics, which may alter content. The journal's standard [Terms & Conditions](#) and the [Ethical guidelines](#) still apply. In no event shall the Royal Society of Chemistry be held responsible for any errors or omissions in this *Accepted Manuscript* or any consequences arising from the use of any information it contains.

Temperature Dependent Iodide Oxidation

by MLCT Excited States

Atefeh Taheri[†] and Gerald J. Meyer^{†§}*

[†]Department of Chemistry, Johns Hopkins University, 3400 North Charles Street,
Baltimore, Maryland, 21218, United States

[§]Department of Chemistry, University of North Carolina at Chapel Hill, Chapel Hill,
North Carolina, 27509, United States

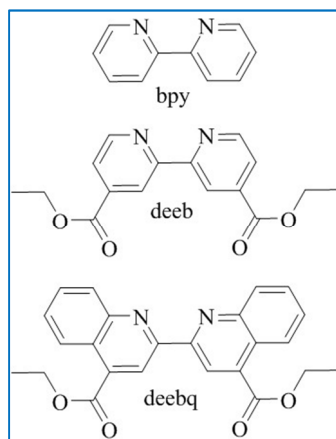
* Email: gjmeyer@email.unc.edu

Abstract

The metal-to-ligand charge transfer (MLCT) excited states of two related heteroleptic Ru(II) compounds $[\text{Ru}(\text{bpy})_2(\text{deeb})]^{2+}$ and $[\text{Ru}(\text{bpy})_2(\text{deebq})]^{2+}$, where bpy is 2,2'-bipyridine, deeb is 4,4'-(CO₂CH₂CH₃)₂-2,2'-bipyridine and deebq is 4,4'-(CO₂CH₂CH₃)₂-2,2'-biquinoline, were characterized in fluid acetonitrile by temperature dependent photoluminescence spectroscopies as well as quenching by iodide ions. Photoluminescence emanates from a manifold of thermally equilibrated excited states referred to as the thexi states. Evidence for activated internal conversion to a 4th MLCT excited state was garnered from an Arrhenius analysis of temperature dependent lifetime data. The activation energy was found to be 550 cm⁻¹ for $[\text{Ru}(\text{bpy})_2(\text{deeb})]^{2+*}$ and 1200 cm⁻¹ for $[\text{Ru}(\text{bpy})_2(\text{deebq})]^{2+*}$. The pre-exponential factor abstracted from the Arrhenius analysis of the $[\text{Ru}(\text{bpy})_2(\text{deebq})]^{2+*}$ data suggested that ligand field excited states might be populated, however there was no evidence for ligand loss photochemistry under the conditions studied. The excited states were found to quench iodide by a dynamic process in good agreement with the Stern-Volmer model. Transient absorption data showed that the quenching mechanism was electron transfer to generate an iodine atom and a reduced ruthenium compound as products. The quenching rate constants abstracted from temperature dependent Stern-Volmer quenching data were corrected for diffusion and activated complex formation to yield electron transfer rate constants that were found to increase markedly with temperature. An Arrhenius analysis of the electron transfer data revealed that electron transfer from iodide to the d-orbitals of the excited state was an activated process with an E_a of 2,400 cm⁻¹ for $[\text{Ru}(\text{bpy})_2(\text{deeb})]^{2+}$ and 3,300 cm⁻¹ for $[\text{Ru}(\text{bpy})_2(\text{deebq})]^{2+}$.

Introduction

In natural photosynthesis, light harvesting and catalysis are physically separated processes.¹ Chlorophyll pigments harvest sunlight and transfer their energy to the ‘special pair’ through the antennae effect which initiates a cascade of electron transfer reactions that ultimately provides redox equivalents to unique and spatially isolated catalytic sites. This physical separation precludes unwanted reactions of the excited state with the catalyst and the catalytic reaction products.¹ However this comes at the entropic expense of precisely orienting the chlorophyll pigments, redox active molecules, and the catalysts. In addition, and perhaps more importantly, much of the free energy stored in the special pair excited state is lost to the electron transfer cascade that precedes catalysis. In principle, more free energy could be utilized for catalysis if the excited state and the catalyst were the same molecule.



Scheme 1. Ligands used in this study.

Catalysis by a molecular excited state has never been realized and remains a goal that could ultimately provide a simple and efficient means to produce solar fuels.² The electronic excited states of transition metal compounds appear to be a good initial starting point for fundamental studies directed toward the realization of this goal.³ In particular, the metal-to-ligand charge-transfer (MLCT) excited state of Ru polypyridyl compounds are particularly attractive.³ Radiative and non-radiative decay from these MLCT excited states is complicated mechanistically by the presence of a number of energy surfaces that can mediate excited state relaxation.⁴⁻¹⁸ Considerable insights into the excited states have been garnered through temperature dependent photophysical studies of

classical compounds like $[\text{Ru}(\text{bpy})_3]^{2+}$, where bpy is 2,2'-bipyridine, and related heteroleptic compounds.⁴⁻¹³ Related studies have also revealed a remarkable sensitivity of the activation barrier(s) for excited state relaxation to the physical environment of the compound.¹⁴⁻¹⁸ In the present study, the excited states of two heteroleptic Ru(II) compounds, $[\text{Ru}(\text{bpy})_2(\text{deeb})]^{2+}$ and $[\text{Ru}(\text{bpy})_2(\text{deebq})]^{2+}$, where deeb is 4,4'-($\text{CO}_2\text{CH}_2\text{CH}_3$)₂-2,2'-bipyridine and deebq is 4,4'-($\text{CO}_2\text{CH}_2\text{CH}_3$)₂-2,2'-biquinoline, Scheme 1, were characterized in fluid acetonitrile solution. In addition, iodide oxidation by these excited states was quantified.

Halide oxidation with solar photons is of considerable interest for the splitting of hydrohalic acids such as HI into hydrogen gas and the elemental halogen.² The thermal oxidation of iodide in fluid solution is known to result in the formation of covalent I-I bonds such as those in I_2 .¹⁹ Prior work has shown that MLCT excited states can oxidize through mechanisms that are dependent upon the molecular details.^{20,21} The reactions that have been studied to date involve ground state ion-pairing between iodide and the transition metal compound²⁰ or diffusional interactions of the excited state with iodide.²¹ In both cases, the chemistry of the excited state is of such critical importance that more detailed characterization is warranted so that desired electron transfer reactions occur quantitatively while in competition with excited state relaxation. To our knowledge this manuscript represents the first temperature dependent study of iodide oxidation by MLCT excited states. Transient absorption studies revealed that iodide oxidation generated an iodine atom that subsequently reacted with a second iodide to form di-iodide, I_2^- . Although the MLCT excited state lifetimes decreased significantly at high temperatures, oxidation was found to be rapid and efficient up to temperatures near the acetonitrile boiling point when high iodide concentrations were employed. The results show that the MLCT excited states can initiate outer-sphere electron transfer reactions that generate I-I bonds that may one day be practically useful in artificial photosynthetic assemblies.

Experimental

Materials. Argon gas (Airgas, 99.99%), tetrabutylammonium iodide (TBAI; Fluka, >99%), triethylamine (TEA; Fisher, 99.9%), and acetonitrile (Burdick & Jackson, spectroscopic grade) were used without further purification. $[\text{Ru}(\text{bpy})_2(\text{deeb})](\text{PF}_6)_2$ and $[\text{Ru}(\text{bpy})_2(\text{deebq})](\text{PF}_6)_2$ were prepared by literature methods.^{20a,22}

Photophysical measurements. *Absorbance Measurements.* Steady-state UV-visible absorption measurements were acquired on a Varian Cary 50 UV-Vis spectrophotometer in a standard 1.00 cm path length quartz cuvette. Transient absorption measurements of all samples were acquired with 532 nm laser excitation (ca. 8 ns full width at half-maximum (fwhm) from a frequency-doubled Nd:YAG Brilliant B Blue Sky laser). A pulsed 150 W Xenon arc lamp (Applied Photophysics) served as the probe beam and was aligned perpendicular to the laser excitation light. Detection was achieved with a monochromator (Spex 1702/04) optically coupled to an R928 photomultiplier tube (Hamamatsu). Transient data over a 60 pulse average were acquired on a computer-interfaced digital oscilloscope (LeCroy 9450, Dual 350 MHz). *Photoluminescence.* Steady-state photoluminescence (PL) measurements were obtained with a fluorimeter (Spex Fluorolog, 1681 spectrometer, 1682 double spectrometer). Lifetime measurements were performed on a GL-3300/GL-301 N₂/dye laser from Photon Technology International. All photophysical measurements were temperature controlled using a liquid nitrogen cryostat (UniSoku CoolSpek USP-203-B) under an argon atmosphere.

Results

The compounds [Ru(bpy)₂(deeb)](PF₆)₂ and [Ru(bpy)₂(deebq)](PF₆)₂ display broad absorption bands in the visible region consistent with metal-to-ligand charge-transfer (MLCT) transitions. Two MLCT absorption bands were observed when [Ru(bpy)₂(deebq)](PF₆)₂ was dissolved in acetonitrile, one at ~ 430 nm and a lower energy band ~ 550 nm. A single structured absorption band centered near 470 nm was observed for [Ru(bpy)₂(deeb)](PF₆)₂. Room temperature photoluminescence (PL) was observed after light excitation of either compound in CH₃CN. A broad featureless PL band centered at 675 nm was measured for [Ru(bpy)₂(deeb)]^{2+*} and at 835 nm for [Ru(bpy)₂(deebq)]^{2+*}. Representative UV-visible absorption and photoluminescence spectral data are given in Figure 1 and are summarized in Table 1.

Excited state relaxation measured after pulsed laser excitation were well described by a first-order kinetic model from which excited state life times, τ_0 , were abstracted at different temperatures from ~ 270 to 320 K. The temperature dependent lifetime data was fit to a modified Arrhenius expression, Equation 1. In this analysis the k_0 value was not fixed and was minimized through a Nelder-Mead modified simplex routine.

$$k = A \exp\left(-\frac{E_a}{k_B T}\right) + k_0 \quad (1)$$

Representative data are given in Figure 2 with additional temperature dependent data give in the Supporting Information. The activation energies and pre-exponential factors are included in Table 1.

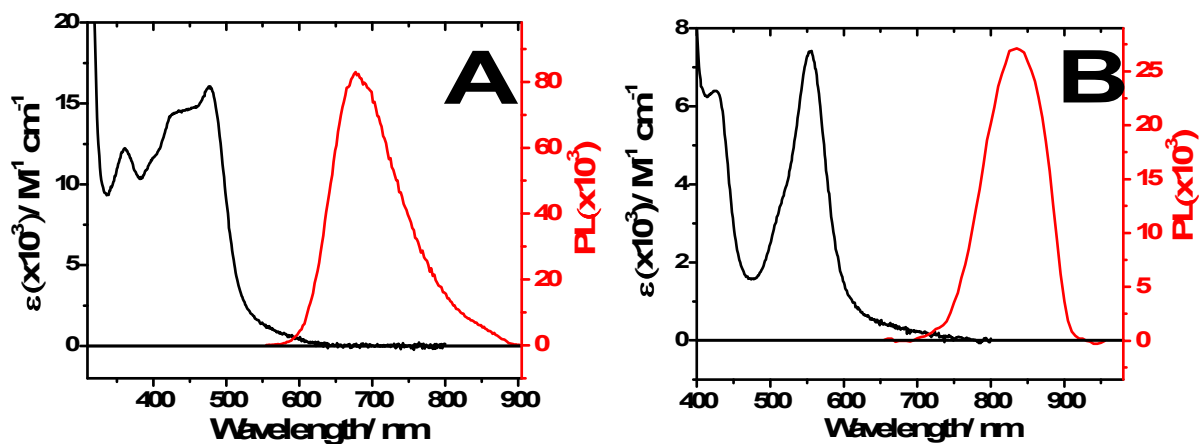


Figure 1. A) Absorption (black) and uncorrected photoluminescence (red) spectra of A) $[\text{Ru}(\text{bpy})_2(\text{deeb})]^{2+}$ and B) $[\text{Ru}(\text{bpy})_2(\text{deebq})]^{2+}$ in CH_3CN at room temperature.

Table 1. Spectroscopic Properties of Ru(II) Compounds in Acetonitrile.

Compound	Abs $\lambda_{\text{max}}/\text{nm}$ ($\epsilon/\text{M}^{-1} \text{cm}^{-1}$) ^a	PL λ_{max} (nm) ^a	τ_0 (ns) ^a	k_0 (s^{-1})	E_a (cm^{-1})	A (s^{-1})
$[\text{Ru}(\text{bpy})_2(\text{deeb})](\text{PF}_6)_2$	478 (16,000)	675	920	8.3×10^5	550	3.6×10^6
$[\text{Ru}(\text{bpy})_2(\text{deebq})](\text{PF}_6)_2$	427 (6,400) 555 (7,400)	835	90	3.7×10^6	1200	2.2×10^9

^aData obtained at 298 K.

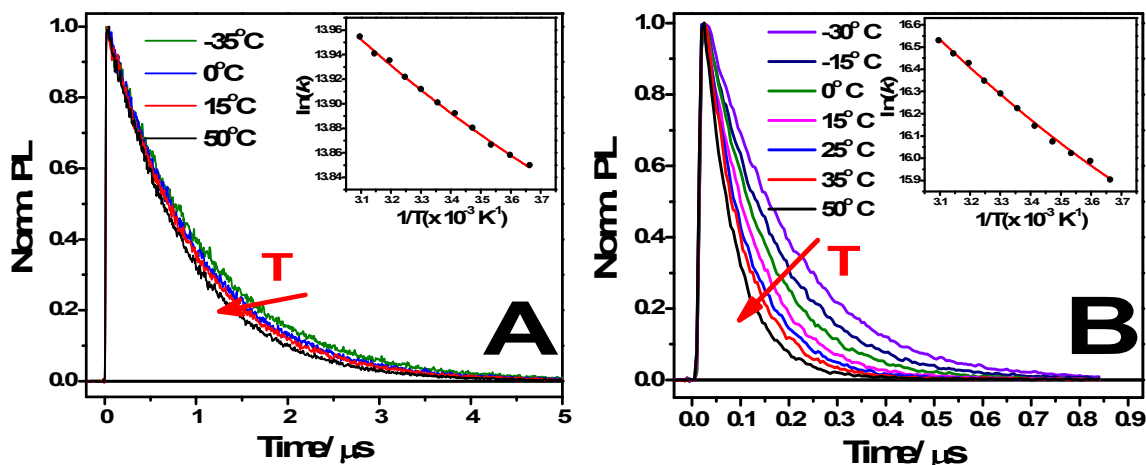


Figure 2. Plots of photoluminescence decay of A) $[\text{Ru}(\text{bpy})_2(\text{deeb})]^{2+}$ B) $[\text{Ru}(\text{bpy})_2(\text{deebq})]^{2+}$ at the indicated temperatures. Insets) Plot of the natural logarithm of the excited state relaxation rate constant versus $1/T$. Overlaid in red are fits to a modified Arrhenius expression, Equation 1.

Figure 3A shows time-resolved PL decays measured after pulsed laser excitation of $[\text{Ru}(\text{bpy})_2(\text{deeb})]^{2+}$ as a function of the iodide concentration in argon purged acetonitrile. Excited-state quenching followed the Stern-Volmer model at all temperatures investigated, from which Stern-Volmer constants, K_{SV} , were abstracted. The kinetic rate constants abstracted from the PL data were in excellent agreement with those measured by transient absorption indicating that the same excited state was probed by these two techniques, Figure 3B. The second-order rate constant for excited-state quenching, k_q , was calculated by the relation $K_{\text{SV}} = k_q \tau_0$ where τ_0 is the excited state lifetime in the absence of iodide. Excited state quenching was found to be more rapid at higher temperatures. For example, k_q increased by a factor of ten from 3.1×10^9 to $3.2 \times 10^{10} \text{ M}^{-1} \text{ s}^{-1}$ as the temperature was raised from 5 to 50°C for $[\text{Ru}(\text{bpy})_2(\text{deeb})]^{2+}$. The quenching rate constants and the excited state lifetimes at the measured temperatures are given in Table 2.

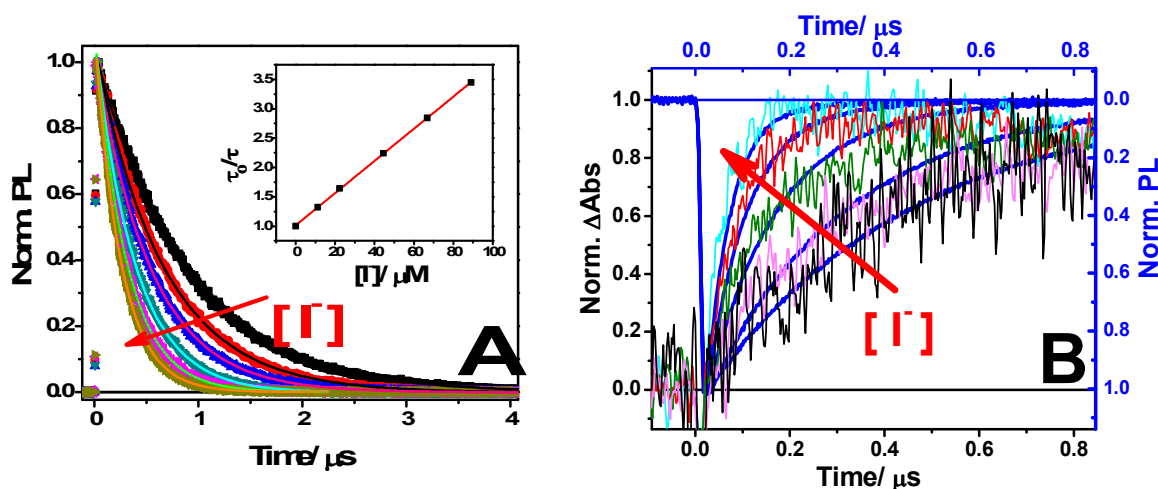


Figure 3. **A)** Time resolved photoluminescence decays monitored at 620 nm for $[\text{Ru}(\text{bpy})_2(\text{deeb})]^{2+*}$ in acetonitrile at 50°C as a function of $[\text{I}^-]$. The insets show the Stern–Volmer plot for lifetime quenching from which $K_{\text{SV}} = 2.7 \times 10^4 \text{ M}^{-1}$ was abstracted. **B)** Representative normalized single wavelength transient absorption data monitored at 528 nm after pulsed laser excitation of $[\text{Ru}(\text{bpy})_2(\text{deeb})]^{2+*}$ in 38 to $750 \mu\text{M}$ iodide solution at 50°C . The time resolved photoluminescence decays monitored at 675 nm (blue) are overlaid on the data.

Table 2. Temperature dependent excited state lifetimes and quenching rate constants by iodide.

Temperature (K)	$[\text{Ru}(\text{bpy})_2(\text{deeb})]^{2+}$		$[\text{Ru}(\text{bpy})_2(\text{deebq})]^{2+}$	
	$\tau_0(\text{ns})$	$k_q(\text{M}^{-1}\text{s}^{-1})$	$\tau_0(\text{ns})$	$k_q(\text{M}^{-1}\text{s}^{-1})$
273	966	-	120	-
278	958	3.1×10^9	115	-
283	950	4.5×10^9	110	6.9×10^9
288	937	5.7×10^9	105	8.7×10^9
293	926	7.8×10^9	97	1.2×10^{10}
298	918	1.0×10^{10}	90	1.2×10^{10}
303	908	1.3×10^{10}	84	1.5×10^{10}
308	899	1.7×10^{10}	79	1.9×10^{10}
313	887	2.2×10^{10}	73	2.3×10^{10}
318	882	2.6×10^{10}	70	2.8×10^{10}
323	870	3.2×10^{10}	66	3.1×10^{10}

Transient absorption spectra were recorded from 380 nm to 780 nm in 10-20 nm increments. Representative data are given in Figure S1. The time dependent concentrations were abstracted from this data through Beer's law with authentic spectra of the reactants, MLCT excited state, the reduced Ru compounds, and $\text{I}_2^{\cdot-}$. The absorption spectra and extinction coefficients of the reduced

compounds were quantified by steady-state photolysis ($\lambda > 400$ nm) of the Ru(II) compounds in argon purged acetonitrile containing 0.1 M triethylamine as has been previously described.²³ Representative data is given in the Supplementary Information Figure S2. The $I_2^{\cdot-}$ spectrum was available from previously published data. Figure 4A shows representative data obtained after pulsed laser excitation of $[Ru(bpy)_2(deeb)]^{2+}$ in 38 μ M and 75 mM TBAI/CH₃CN solutions at 50° C. Overlaid on this data are normalized PL decays that the first-order kinetics for excited state relaxation are within experimental error the same as that for the appearance of the reduced ruthenium compound, $[Ru(bpy)_2(deeb^{\cdot-})]^+$. In contrast, the formation of $I_2^{\cdot-}$ was significantly slower, behavior that was most evident for the 38 μ M iodide concentration in Figure 4A where the growth was not complete within the 2.5 microseconds shown. Figure 4B shows that the rate at which $[Ru(bpy)_2(deeb^{\cdot-})]^+$ was produced after laser excitation increased dramatically when the temperature was raised from 0° to 50°C.

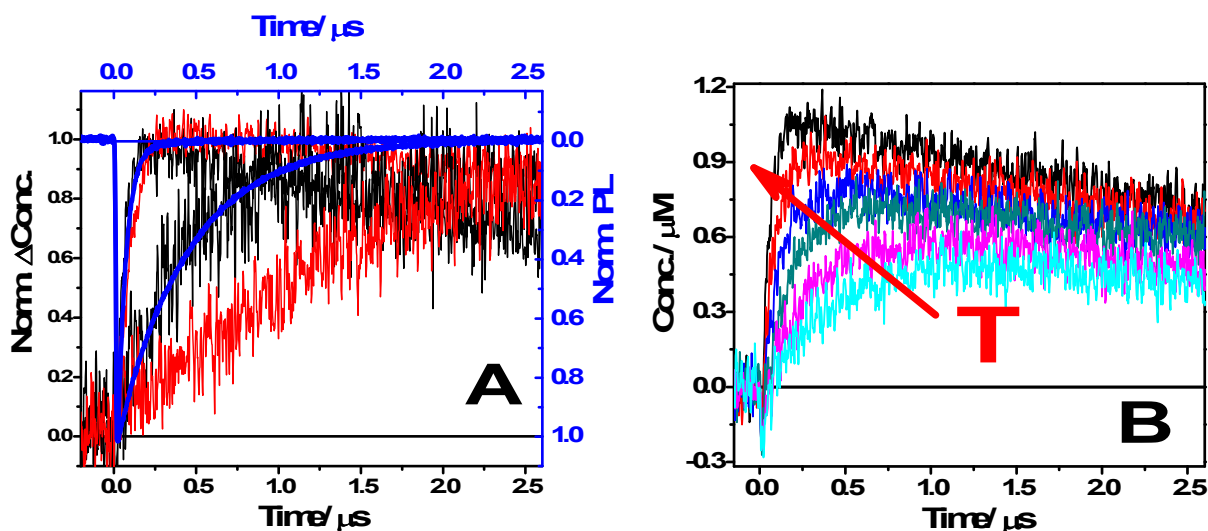


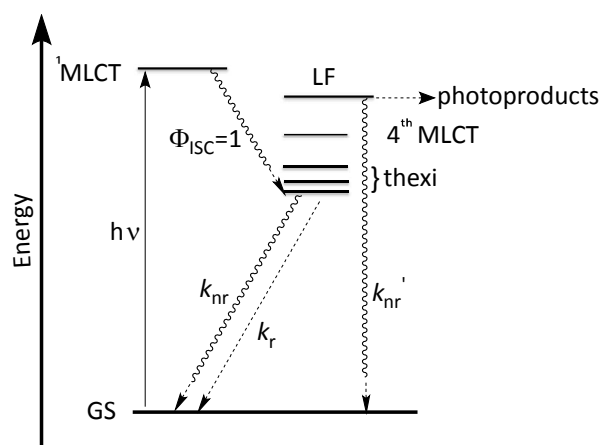
Figure 4. **A)** Time dependent concentration of $[Ru(bpy)_2(deeb^{\cdot-})]^+$ (black) and $I_2^{\cdot-}$ (red) after 532 nm excitation of $[Ru(bpy)_2(deeb)]^{2+}$ in 38 μ M and 75 mM iodide/CH₃CN solutions at 50° C; the longer lived transients represent the lower 38 μ M iodide concentration. Overlaid in blue are normalized time resolved PL decay monitored at 600 nm for the two iodide concentrations. **B)** Time dependent concentration of $[Ru(bpy)_2(deeb^{\cdot-})]^+$ after 532 nm excitation of $[Ru(bpy)_2(deeb)]^{2+}$ in a 75 mM iodide/CH₃CN solutions from 0° to 50° C.

Discussion

The temperature dependent photophysical studies of the two heteroleptic Ru(II) compounds has provided some new insights into MLCT excited state relaxation and the reactivity of the MLCT state for iodide oxidation. Below the spectroscopic characterization of the excited states is discussed within the broader context of the published literature followed by the iodide oxidation chemistry.

MLCT Excited States

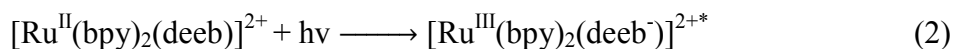
The classical studies of Crosby and coworkers established that the photoluminescence from $[\text{Ru}(\text{bpy})_3]^{2+*}$ emanates from three electronic states separated in energy by only 40 cm^{-1} .⁴ Crosby assigned a symmetry label to the excited state point group without designating a spin because spin-orbit coupling by the heavy Ru center makes spin a poor quantum number.^{4b} These three states have significant Boltzmann population near room temperature and hence behave as a single state that is often referred to as the ‘thermally equilibrated’ or ‘thexi’ state. Studies by TJ Meyer and coworkers revealed a 4th MLCT excited state that accounted for the weak temperature dependence near room temperature.⁵ Higher in energy are the so-called ligand field or d-d states that are anti-bonding with respect to metal-ligand bonds. A Jablonski type diagram that incorporates these electronic states is shown in Scheme 2. While such a diagram is based on $[\text{Ru}(\text{bpy})_3]^{2+}$, it is often applied to other Ru(II) compounds of lower symmetry.



Scheme 2. Jablonski type diagram for $[\text{Ru}(\text{bpy})_3]^{2+}$.

The $[\text{Ru}(\text{bpy})_3]^{2+}$ has D_3 symmetry. If one ignores the ester groups, replacement of the bpy with a deeb or deebq ligand lowers the symmetry to approximately C_2 . Light excitation generates a

Franck-Condon state that crosses to a thexi state with an electron localized on a single ligand on a femtosecond time scale.²⁴ For heteroleptic compounds, the electron localizes on the ligand with the lowest lying π^* orbitals.³ Previous studies have shown that the π^* orbitals decrease in energy in the following order: bpy > deeb > deebq.²² This ordering is most apparent in the absorption spectrum of $[\text{Ru}(\text{bpy})_2(\text{deebq})]^{2+}$ where the higher energy absorption band was Ru \rightarrow bpy charge-transfer (\sim 430 nm) and the lower energy band (\sim 550 nm) was Ru \rightarrow deebq charge transfer as was confirmed by resonance Raman spectroscopy.²² The Ru \rightarrow bpy and Ru \rightarrow deeb MLCT transitions in $[\text{Ru}(\text{bpy})_2(\text{deeb})]^{2+}$ were close in energy giving rise to a single structured absorption band centered near 470 nm. Evolution of the Franck Condon state to the thexi state is expected to occur on a femtosecond time scale such that the excited state probed in these nanosecond experiments is reasonably assigned as a Ru center coordinated to two bipyridine ligands and a reduced diimine ligand with the formal oxidation states given in Equations 2 and 3.²⁴ Due to significant mixing of metal- t_{2g} and ligand- π^* orbitals in the THEXI state, the formality of the Ru^{III} oxidation state should be regarded with caution.³ Unlike $[\text{Ru}(\text{bpy})_3]^{2+}$, the ground and thexi states are expected to have the same C_2 symmetry.



The $[\text{Ru}(\text{bpy})_2(\text{deeb})]^{2+*}$ MLCT excited state was approximately ten times longer lived than was the corresponding biquinoline compound. A shorter excited state lifetime was expected for $[\text{Ru}(\text{bpy})_2(\text{deebq})]^{2+*}$ as the ground state-excited state energy gap was much smaller, 1.99 vs. 1.64 eV. MLCT excited states are known to follow Jortner's energy gap law where the non-radiative rate constant increases exponentially as the energy gap decreases as was qualitatively observed here.²⁵ Raman studies where the excitation wavelength was resonant with the Ru \rightarrow deeb or Ru \rightarrow deebq MLCT states, showed no enhancement of the ethyl ester vibrational modes.²² This indicated that the esters are poorly conjugated with the aromatic pyridine/quinoline rings in the ground state, and are perhaps orthogonal to them. On the basis of the fact that $[\text{Ru}(\text{bpy})_2(\text{deeb})]^{2+*}$ has a longer lifetime than does $[\text{Ru}(\text{bpy})_3]^{2+*}$ even though the deeb containing compound has a smaller energy gap, it is tempting to assert that the ester functional groups twist in the excited state to become more aligned

with the ligand π^* orbitals in the excited state. This would lead to greater delocalization of the excited state and a long lifetime consistent with the data. While such excited state reorganization is speculative for these compounds, McCusker and coworkers have provided compelling evidence that phenyl rings in the 4 and 4'-positions of bipyridine do indeed twist and become more co-planar with the pyridine rings in the thexi state of related Ru(II) polypyridyl compounds.²⁶

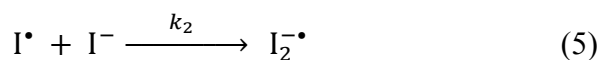
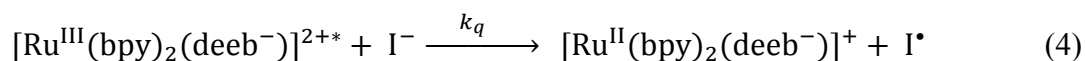
Typically, thexi \rightarrow LF internal conversion is associated with a pre-exponential factor of 10^{10} - 10^{14} s⁻¹ and an activation energy of 2,000-4,000 cm⁻¹, while population of the 4th MLCT state has pre-exponential factor of 10^4 - 10^6 s⁻¹ and an activation energy of 200-600 cm⁻¹. Analysis of the temperature dependent lifetimes for [Ru(bpy)₂(deeb)]^{2+*} revealed an activation energy of 550 cm⁻¹ and a pre-exponential factor of 4×10^6 s⁻¹. Based on previous studies, this is reasonably assigned to relaxation through the 4th MLCT excited state.⁵ The activation energy measured for [Ru(bpy)₂(deebq)]^{2+*} was 1200 cm⁻¹ with a pre-exponential factor of 2×10^9 s⁻¹, which is also assigned to the 4th MLCT excited state, although the pre-exponential term is somewhat larger than would be expected. The thexi state of [Ru(bpy)₂(deebq)]^{2+*} is lower in energy than that for the deeb analogue and if the energy of the 4th MLCT state were the same for the two compounds, a larger energy gap would be expected. Alternatively, the [Ru(bpy)₂(deebq)]^{2+*} data may reflect an 'average' of ligand field and 4th MLCT state population that cannot be fully separated experimentally due to the limited temperature range of the acetonitrile solvent. X-ray crystallographic studies of [Ru(bpy)₂(deebq)]²⁺ revealed that the Ru-N biquinoline bonds were longer than the Ru-N bipyridine bonds.²² The H atoms closest to N on the biquinoline ligand interact unfavorably with the two bipyridine ligands in an octahedral geometry and the resultant steric interactions presumably underlie the longer bond length. A long bond is generally a weak bond that implies a smaller ligand field splitting for the biquinoline compared to bipyridine. This suggests that the LF states may be more accessible to the [Ru(bpy)₂(deebq)]^{2+*} than for [Ru(bpy)₂(deeb)]^{2+*}.

Recall that the LF states are anti-bonding with respect to M-L bonds and population results in ligand loss photochemistry. No significant photochemistry was observed for [Ru(bpy)₂(deebq)]^{2+*} as was judged by steady state absorption measurements made before and after variable temperature photophysical studies. However, the chelate effect may mask any Ru-N bond breakage as coordination to the other N atom facilitates efficient reformation of the broken Ru-N bond. It should be noted that significant ligand loss photochemistry has been reported for Ru compounds with two or three biquinoline ligands.²⁷ The temperature dependent photophysical studies here are consistent

with photochemically stable compounds that undergo deactivation through a 4th MLCT excited state even at elevated temperatures.

Excited State Iodide Oxidation

Photoluminescence quenching is an indirect technique for the study of light driven electron transfer. For this reason transient absorption studies were performed to quantify the mechanism. The data provided give compelling evidence that excited state iodide oxidation yields an iodine atom, Equation 4. The iodine atom subsequently reacts with iodide to form an I-I bond in di-iodide, I₂^{•-}, Equation 5.

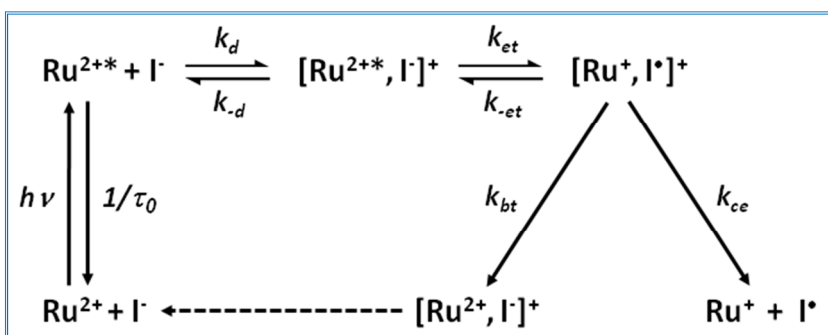


Hence the quenching process involves electron transfer from iodide to the d-orbitals of the MLCT excited state. The excited state reduction potentials of the compounds were estimated from the measured ground state reduction potentials and the photoluminescence spectra as has been previously described.²⁸ Based on an E^o(I⁻/I[•]) of 0.99 V vs. NHE,²⁹ the free energy change for the reaction with [Ru(bpy)₂(deeb)]^{2+*} is 0 and is -40 meV for [Ru(bpy)₂(deebq)]^{2+*}. The larger driving force for the reaction with the biquinoline compound was reflected by quenching rate constants that were significantly larger than those for [Ru(bpy)₂(deeb)]^{2+*}.

The kinetic data provided clear evidence that the reduced Ru compound appeared with the same rate constant as did the disappearance of the MLCT excited state demonstrating that it was a primary photochemical reaction product. The formation of I₂^{•-} was consistently slower indicating that it was not a primary photochemical product. Instead the iodine atom was the presumed primary reaction product that subsequently reacted with iodide to yield I₂^{•-}. The rate constant for the reaction of iodine atom and iodide, k₂, was previously reported to be 2.4 × 10¹⁰ M⁻¹ s⁻¹ at room temperature in acetonitrile in good agreement with the value measured here.^{20b} The coincidence of these rate constants provides compelling evidence that the iodine atom, that was not spectroscopically observed, was indeed the primary reaction product.

The measured quenching constant, k_q, includes contributions from diffusion, k_{diff}, electron-transfer steps, k_{et}, and formation of an encounter complex, K_A. Often one is most interested in the electron transfer rate constants and the energy barriers that may be associated with it.³⁰ Fortunately,

bimolecular electron transfer reactions are well known and at least in principle the true electron transfer rate constants can be abstracted from the excited state quenching data. To accomplish this an intimate mechanism for the reaction is proposed, Scheme 3.



Scheme 3. Intimate mechanism for MLCT excited state iodide oxidation.

Electron-transfer occurs by diffusion of the MLCT excited state, abbreviated as Ru^{2+*} , and iodide to generate an encounter complex, $[\text{Ru}^{2+*}, \text{I}]^+$ with an equilibrium constant defined by $K_A = k_d/k_{-d}$. Electron-transfer within the encounter complex occurred based upon the equilibrium constant $K_{et} = k_{et}/k_{-et}$ established by the Gibb's free-energy for electron-transfer using the exact relation $K_{et} = \exp(-\Delta G^\circ/RT)$. Finally, cage escape of the electron-transfer products (k_{ce}) yielded solvent separated species in the form of Ru^+ and I^* . It was previously shown that the yield of separated products was typically $\phi_{ce} < 5\%$ with no clear dependence on the driving force for electron-transfer.^{21a} Poor cage escape yields represent a significant disadvantage of using excited states for catalysis and may contribute to Nature's evolutionary choice to use redox equivalents to drive catalysis that avoids highly favorable back electron transfer to yield ground-state products (k_{bt}) within the encounter complex.

According to Scheme 3, the observed second-order rate constants for iodide oxidation to the iodine atom, k_q , are defined by the rate constants for activated complex formation and the forward electron-transfer rate constant, Equation 6. For bimolecular rate constants, $K_A k_{et}$ is often referred to concisely as the activation rate constant, k_{act} , and has second-order units of $\text{M}^{-1} \text{s}^{-1}$.³⁰

$$\frac{1}{k_q} = \frac{1}{k_{diff}} + \frac{1}{K_A k_{et}} \quad (6)$$

The rate constants for diffusion were estimated based upon the Debye-Smoluchowski relation, Equation 7. In this equation N_A is Avogadro's number and D_1 and D_2 are the diffusion coefficients for Ru^{2+*} and Γ and are calculated by the Stoke-Einstein equation, $D = (k_B T / 6 \pi \eta r)$ where η is the viscosity of the solvent and r is radius of the species. A value of 2.2 Å was utilized for the iodide radius. An ellipsoidal space filling model yielded values of 6.84 and 7.07 Å for $[\text{Ru}(\text{bpy})_2(\text{deeb})]^{2+*}$, and $[\text{Ru}(\text{bpy})_2(\text{deebq})]^{2+*}$, respectively. The values of η from - 40 to + 50°C for acetonitrile have been reported experimentally.³¹ The diffusion rate constants were consistently at least a factor of four larger than the measured k_q values. The effective reaction radius, β , is defined by Equation 8. This term adjusts the sum of the ionic radii, by accounting for ionic interactions through the Onsager radius, $R_c = (z_1 z_2 e^2 / 4 \pi \epsilon_r \epsilon_0 k_B T)$, and the Debye length, $\kappa = (2000 e^2 N_A I / \epsilon_r \epsilon_0 k_B T)^{1/2}$. In these two parameters, I is the ionic strength and all other terms retain their normal meaning. An empirical relation, $\ln \epsilon = 3.579 + 1.163 \times 10^3 \times T - 5.5 \times 10^6 T^2$, was used to calculate the dielectric constant, ϵ , at all temperatures for acetonitrile.³² The diffusion rate constants were consistently at least a factor of four smaller than the measured k_q values. The association equilibrium constants, K_A were estimated with Equation 9.^{30,33}

$$k_{diff} = 4 \pi N_A (D_1 + D_2) \beta \quad (7)$$

$$\beta = \frac{R_c}{(\exp(\frac{R_c}{R}) - 1)} \exp(R_c \kappa) \quad (8)$$

$$K_A = N_A 1000 \left(\frac{4}{3}\right) \pi R^3 \exp\left(\frac{-R_c}{R}\right) \quad (9)$$

With this approach, the measured k_q values were 'corrected' to yield the true excited state electron transfer rate constants, k_{et} . An Arrhenius analysis of this data is shown in Figure 5. The pre-exponential factors were in the 10^{13} - 10^{15} s^{-1} range and the activation energies were significant, $E_a = 2,400 \text{ cm}^{-1}$ and $3,300 \text{ cm}^{-1}$ for $[\text{Ru}(\text{bpy})_2(\text{deebq})]^{2+}$ and $[\text{Ru}(\text{bpy})_2(\text{deeb})]^{2+}$, respectively. The barrier is related to transition from the encounter complex to the transition state, neither of which are known experimentally. Previous NMR studies have shown that halides in dichloromethane preferentially interact with the 3 and 3' hydrogen atoms of bipyridine ligands.³⁴ These H atoms are the most acidic and represent the most probable sites of halide interaction in any solvent. Assuming that iodide forms an adduct with the 3 and 3'-H atoms of bipyridine in the encounter complex, the electron from

iodide must traverse $\sim 3 \text{ \AA}$ to the Ru metal center. The larger barrier for the $[\text{Ru}(\text{bpy})_2(\text{deeb})]^{2+*}$ excited state is hard to rationalize based on this encounter complex geometry as the ester containing ligands is remote to the proposed electron transfer pathway. Nevertheless, the data clearly shows that iodide oxidation is activated and studies with a wider variety of Ru(II) compounds would be expected to provide more insights into the nature of the encounter complex and the transition state.

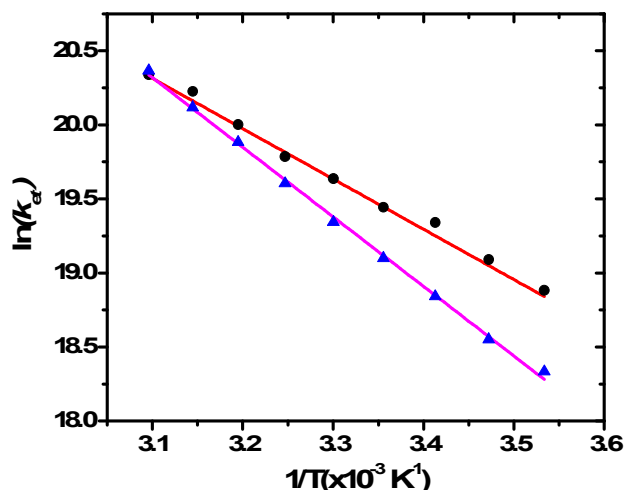


Figure 5. Plots of $\ln(k_{\text{et}})$ vs. $1/T$ for $[\text{Ru}(\text{bpy})_2(\text{deebq})]^{2+}$ (black circles) and $[\text{Ru}(\text{bpy})_2(\text{deeb})]^{2+}$ (blue triangles) acquired from iodide excited-state quenching data measured in acetonitrile. Overlaid lines are linear fits that yielded activation energies of 2400 cm^{-1} and 3300 cm^{-1} for $[\text{Ru}(\text{bpy})_2(\text{deebq})]^{2+}$ and $[\text{Ru}(\text{bpy})_2(\text{deeb})]^{2+}$, respectively.

Conclusions

The metal-to-ligand charge transfer (MLCT) excited states of $[\text{Ru}(\text{bpy})_2(\text{deeb})]^{2+}$ and $[\text{Ru}(\text{bpy})_2(\text{deebq})]^{2+}$ were sufficiently long-lived to undergo efficient diffusional electron transfer with iodide in fluid acetonitrile over a 40° temperature range. Analysis of the temperature dependent lifetimes of the MLCT excited states revealed activation parameters consistent with previous reports for activated internal conversion to a 4th MLCT excited state. No clear evidence for population of ligand field excited states was obtained, behavior consistent with the high photochemical stability of these compounds. The MLCT excited states were efficiently quenched by iodide to yield an iodine atom and a reduced ruthenium compound as products. The quenching rate constants were corrected for diffusion and activated complex formation to yield electron transfer rate constants that increased markedly with temperature. This data showed for the first time that electron

transfer from iodide to the excited state was activated with an activation energy of 2,400 cm⁻¹ for [Ru(bpy)₂(deeb)]²⁺ and 3,300 cm⁻¹ for [Ru(bpy)₂(deebq)]²⁺. The data suggest that these excited states can one day be utilized for solar light harvesting *and* iodide oxidation catalysis.

ACKNOWLEDGMENTS

The Division of Chemical Sciences, Geosciences, and Biosciences, Office of Basic Energy Sciences of the U.S. Department of Energy through Grant DE-FG02-96ER14662 is gratefully acknowledged for support.

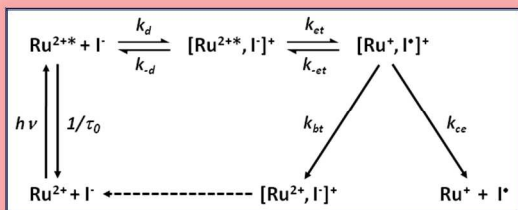
References

1. Blankenship, R.E. (2008). *Molecular Mechanisms of Photosynthesis* (2nd ed.). John Wiley & Sons Inc.
2. Lewis, N. S.; Nocera, D. G. *Proc. Natl. Acad. Sci. U. S. A.* **2006**, *103* (43), 15729-15735.
3. Kalyanasundaram, K. (1992). *Photochemistry of polypyridine and porphyrin complexes*. Boston: Academic Press.
4. (a) Demas, J. N.; Crosby, G. A. *J. Am. Chem. Soc.* **1971**, *93* (12), 2841-2847. (b) Crosby, G. A.; Hipps, K. W.; Elfring, W. H. *J. Am. Chem. Soc.* **1974**, *96* (2), 629-630. (c) Hager, G. D.; Watts, R. J.; Crosby, G. A. *J. Am. Chem. Soc.* **1975**, *97* (24), 7031-7037. (d) Hager, G. D.; Watts, R. J.; Crosby, G. A. *J. Am. Chem. Soc.* **1975**, *97* (24), 7037-7042.
5. Lumpkin, R. S.; Kober, E. M.; Worl, L. A.; Murtaza, Z.; Meyer, T. J. *J. Phys. Chem.* **1990**, *94*, 239-243
6. Sykora, M.; Kincaid, J. R. *Inorg. Chem.* **1995**, *34* (23), 5852-5856.
7. Alary, F.; Heully, J. L.; Bijeire, L.; Vicendo, P. *Inorg. Chem.* **2007**, *46* (8), 3154-3165.

8. (a) Pinnick, D. V.; Durham, B. *Inorg. Chem.* **1984**, *23* (10), 1440-1445. (b) Pinnick, D. V.; Durham, B. *Inorg. Chem.* **1984**, *23* (24), 3841-3842.
9. (a) Wright, D. W.; Schmehl, R. H. *Inorg. Chem.* **1990**, *29* (2), 155-157. (b) Wacholtz, W. M.; Auerbach, R. A.; Schmehl, R. H.; Ollino, M.; Cherry, W. R. *Inorg. Chem.* **1985**, *24* (12), 1758-1760. (c) Reveco, P.; Schmehl, R. H.; Cherry, W. R.; Fronczek, F. R.; Selbin, J. *Inorg. Chem.* **1985**, *24* (24), 4078-4082. (d) Wacholtz, W. M.; Auerbach, R. A.; Schmehl, R. H. *Inorg. Chem.* **1986**, *25* (2), 227-234.
10. (a) Chaisson, D. A.; Hintze, R. E.; Stuermer, D. H.; Petersen, J. D.; McDonald, D. P.; Ford, P. C. *J. Am. Chem. Soc.* **1972**, *94* (19), 6665-6673. (b) Malouf, G.; Ford, P. C. *J. Am. Chem. Soc.* **1977**, *99* (22), 7213-7221.
11. Barigelletti, F.; Juris, A.; Balzani, V.; Belser, P.; Von Zelewsky, A. *J. Phys. Chem.* **1987**, *91* (5), 1095-1098.
12. Allsopp, S. R.; Cox, A.; Kemp, T. J.; Reed, W. J. *J. Chem. Soc., Faraday Trans.* **1978**, *74*, 1275-1289.
13. Liu, Y.; Turner, D.B.; Singh, T.N.; Angeles-Boza, A.M.; Chouai, A.; Dunbar, K.R.; Turro, C. *J. Am. Chem. Soc.* **2009**, *131*, 26-27.
14. Fan, J.; Tysoe, S.; Streckas, T. C.; Gafney, H. D.; Serpone, N.; Lawless, D. *J. Am. Chem. Soc.* **1994**, *116* (12), 5343-5351.
15. (a) Maruszewski, K.; Strommen, D. P.; Kincaid, J. R. *J. Am. Chem. Soc.* **1993**, *115*, 8345-8350. (b) Maruszewski, K.; Kincaid, J. R. *Inorg. Chem.* **1995**, *34* (8), 2002-2006.
16. Masschelein, A.; Mesmaeker, A. K.-D.; Willsher, C. J.; Wilkinson, F. *J. Chem. Soc., Faraday Trans.* **1991**, *87* (2), 259-267.
17. Qu, P.; Thompson, D. W.; Meyer, G. J. *Langmuir* **2000**, *16*, 4662-4671.

18. (a) Chen, P.; Meyer, T. J. *Chem. Rev.* **1998**, *98* (4), 1439-1478. (b) Thompson, D. W.; Fleming, C. N.; Myron, B. D.; Meyer, T. J. *J. Phys. Chem. B* **2007**, *111* (24), 6930-6941.
19. (a) Nord, G. *Comments Inorg. Chem.* **1992**, *13*, 221-239; (b) Hung, M.-L.; McKee, M. L.; Stanbury, D. M. *Inorg. Chem.* **1994**, *33*, 5108-5112.
20. (a) Clark, C. C.; Marton, A.; Meyer, G. J. *Inorg. Chem.* **2005**, *44*, 3383-3385; (b) Marton, A.; Clark, C.C.; Srinivasan, R.; Freundlich, R.E.; Narducci-Sarjeant, A.A.; Meyer, G.J. *Inorg. Chem.* **2006**, *45*, 362-369. (c) Farnum, B. H.; Gardner, J. M.; Marton, A.; Narducci-Sarjeant, A. A.; Meyer, G. J. *Dalton Trans.* **40** (15), 3830-3838. (d) Rowley, J. G.; Farnum, B. H.; Ardo, S.; Meyer, G. J. *J. Phys. Chem. Lett.* **2010**, *1* (20), 3132-3140.
21. (a) Gardner, J.M.; Giaimuccio, J.M.; Meyer, G.J. *J. Am. Chem. Soc.* **2008**, *130*, 17252-17253. (b) Gardner, J. M.; Abrahamsson, M.; Farnum, B. H.; Meyer, G. J. *J. Am. Chem. Soc.* **2009**, *131* (44), 16206-16214. (c) Farnum, B. H.; Jou, J. J.; Meyer, G. J. *Proc. Natl. Acad. Sci. U. S. A.* **2012**, *109* (39), 15628-15633.
22. Hoertz, P. G.; Staniszewski, A.; Marton, A.; Higgins, G. T.; Incarvito, C. D.; Rheingold, A. L.; Meyer, G. J. *J. Am. Chem. Soc.* **2006**, *128* (25), 8234-8245.
23. DeLaive, P. J.; Sullivan, B. P.; Meyer, T. J.; Whitten, D. G. *J. Am. Chem. Soc.* **1979**, *101* (14), 4007-4008.
24. Yeh, A. T.; Shank, C. V.; McCusker, J. K. *Science* **2000**, *289* (5481), 935-938.
25. Englman, R.; Jortner, J. *Mol. Phys.* **1970**, *18* (2), 145-152.
26. (a) Damrauer, N. H.; Boussie, T.R.; Devenney, M.; McCusker, J. K. *J. Am. Chem. Soc.*, **1997**, *119* (35), 8253-8268. (b) Damrauer, N. H.; McCusker, J. K. *J. Phys. Chem. A* **1999**, *103* (42), 8440-8446.
27. Von Zelewsky, A.; Gremaud, G. *Helv. Chim. Acta* **1988**, *71*, 1108-1122.

28. Rehm, D.; Weller, A. *Isr. J. Chem.* **1970**, *8*, 259-266.
29. Wang, X. G.; Stanbury, D. M. *Inorg. Chem.* **2006**, *45* (8), 3415-3423.
30. Sutin, N. *Acc. Chem. Res.* **1982**, *15* (9), 275–282.
31. Janz, G. R.; Tomkins, R. P. *Nonaqueous Electrolytes Handbook*, Academic Press: *Yew York* **1972**, *1*.
32. Wurflinger, A. *Ber. Bunsen-Ges. Phys. Chem. Chem. Phys.* **1980**, *84* (7), 653-657.
33. Crowley, C. E.; Clark, C. D.; Hoffman, M. Z. *Inorg. Chem.* **1998**, *37*, 5704-5706.
34. Ward, W. M.; Farnum, B. H.; Siegler, M.; Meyer, G. J. *J. Phys. Chem. A* **2013**, *117* (36), 8883-8894.



Temperature dependent excited state iodide oxidation by two heteroleptic Ru polypyridyl compounds was quantified for the first time.